

Modeling and Control of a 50KW Electric Vehicle Fast Charger

Alon Kuperman,
Ariel University
Center of Samaria

Udi Levy,
Gamatronic
Electronic
Industries, LTD

Joseph Goren,
Gamatronic
Electronic
Industries, LTD

Aryeh Zafranski,
Gamatronic
Electronic
Industries, LTD

Alex Savernin,
Gamatronic
Electronic
Industries, LTD

Ilan Peled
Better Place,
Inc.

Abstract— Modeling and control of a 50KW vehicle battery fast charger prototype, developed at Gamatronic Electronic Industries LTD, is presented in the paper. The charger topology may be referred as a two-stage controlled rectifier. The input stage consists of a three phase full bridge rectifier combined with an active power filter (three single stage power filters are actually employed). The input stage creates an uncontrolled DC bus while complying with the grid codes by keeping the THD and power factor within the permissible limits. The output stage is formed by six interleaved groups of two DC-DC converters, reducing the input and output current ripples. Two independent control boards are employed: active filters control circuitry and the DC-DC control circuitry. The former is operated according to the predetermined grid interfacing behavior, while the operation of the latter is dictated by the requests from the Battery Management System. The charger is capable of operating in any of the two modes: Constant Current and Constant Voltage. Control loops are explained throughout the paper and extended simulation/experimental results are presented.

I. INTRODUCTION

The traction battery (typically of the lithium-ion type) is undoubtedly the most critical component of an electric vehicle (EV), since the cost, the weight as well as the reliability and driving range of the vehicle are strongly influenced by the battery characteristics [1], [2]. Moreover, the battery must be properly managed, and in particular properly recharged in order to utilize its full capacity and preserve its nominal lifetime [3] – [6].

There are two types of battery chargers: the on-board (sometimes called slow or low power) charger, through which the battery is recharged when parking and plugged into a charging spot [7] – [14], and the off-board (so-called fast or high power) charger, located at the Battery Switch Station (BSS) [15], [16]. The slow charger usually operates at 0.1–0.2C rates, while the fast charger rate typically reaches 1–2C rates, i.e. while charging a 25KWh battery; the slow charger supplies 3–4KW while the fast charger peak power is around 30–50KW. The typical concept of EV includes urban driving

only, where the full battery charge is sufficient for short-range routes. Recharging is accomplished by plugging the car into charge spots placed at different city locations throughout the day and at driver's home during the night. Recently, a paradigm shift towards closing the gap between EV and conventional vehicles has occurred, forcing the infrastructure to support EV intercity driving as well. The following concept of BSS was developed: when out of charge, the EV battery can be replaced at a BSS, allowing nearly uninterrupted long range driving. The near-empty battery, removed from a vehicle at the BSS, is charged by a fast charger (FC), and is available as quickly as possible for the next customer.

The FC is basically a controlled AC/DC power supply, drawing the power from the three phase AC utility grid and injecting it into the traction battery. In order to provide a feasible solution, the FC must satisfy both the grid code in terms of THD and power factor from the utility side and lithium-ion charging modes from the battery side.

Since the BSS usually contains multiple FCs, its impact on the distribution grid is very significant, as was shown by previous research [17]–[23]. Therefore, the input stage of the FC usually performs rectification and power factor correction (PFC) according to the regulation requirements. It can be accomplished either by employing an active rectifier [24]–[26], or a diode rectifier combined with a PFC circuit. The well-known single phase PFC approach, where a full-rating boost DC-DC converter follows the diode rectifier [27] is unsuitable for the three-phase case. However, it can either be modified by splitting the three-phase rectifier into two single-phase legs followed by two independent PFC converters [28]. Alternatively, a more elegant approach employs a shunt connected active power filter (APF) at the rectifier input, supplying the reactive current to the diode rectifier and thus achieving both near unity power factor and near zero THD by forcing the utility to supply the active current, which is in phase with the utility voltage and of the same shape [29]–[35]. The use of either one three phase [29] – [32] or three single phase [33]–[35] APF configurations are potentially feasible for implementing a three phase PFC. The additional advantage of the approach is the fact that because of the shunt connection, the APF rating is approximately 40% of the

series-connected PFC circuit rating, since the APF supplies the reactive power only to the diode rectifier (which is around 40% of the active power, flowing through the rectifier), while the series connected PFC converter supplies the active power, demanded by the load.

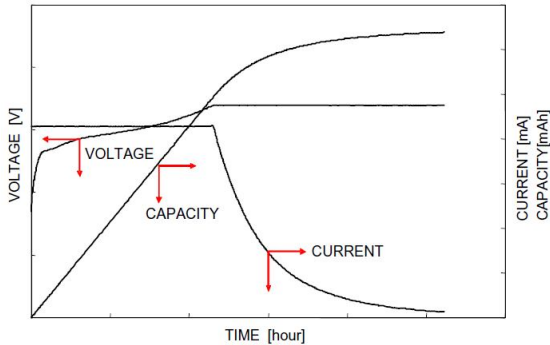


Fig. 1: Lithium-ion battery charging modes

A lithium-ion battery charging is characterized by two main phases: constant current (CC) and constant voltage (CV), as shown in Fig. 1. The battery is charged by a constant current until the voltage reaches a predetermined level. From this point the voltage is kept constant while the current reduces as the capacity approaches 100%. Hence, the charger output stage must be capable of operating either as a current source or as a voltage source. Alternatively, it can be operated as a voltage supply with dynamic current limitation. In addition, the charger output current ripple should be kept as low as possible in order to prevent undesired influence on the battery chemistry. The well-known approach, allowing splitting the load power between multiple modules in order to reduce the conduction losses and current ripple is interleaving [36], [37]. Interleaving employs parallel operation of converters, whose output current is shifted with respect to others such that when summed, the current ripples partially cancel each other to create a low ripple total output current. It also reduces the implementation challenge of designing a single full rating converter by using several lower rating converters instead.

The paper describes modeling and control of a 50KW FC, employing a three phase diode rectifier combined with three single phase APFs as the input stage and twelve buck DC-DC converters, divided into six interleaved groups as the output

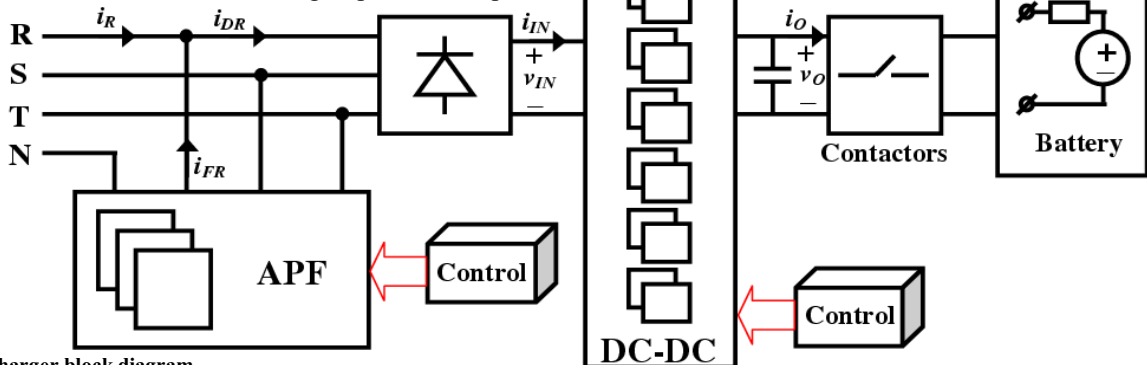


Fig. 2: Fast charger block diagram

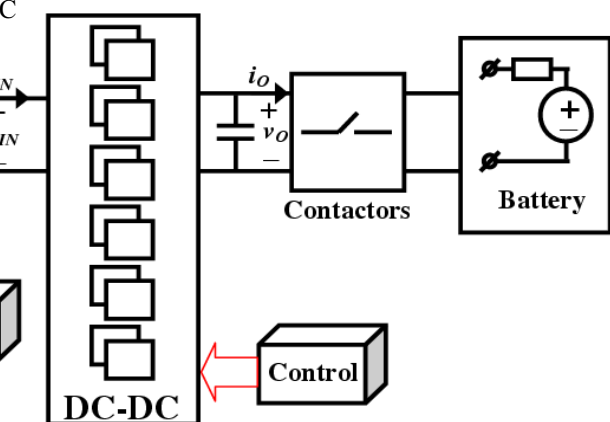
stage. The charger operates as a voltage supply with controllable dynamic current limitation. The charger operates from the 380V three phase utility grid and is able to charge lithium-ion batteries within the voltage range of 230 - 430V by supplying 0 – 125A current.

The rest of the paper is organized as follows. Section II presents the FC overview. The input stage operation is presented in Section III, followed by the output stage description, given in Section IV. Extended simulation results are shown in Section V. The paper is concluded in Section VI.

II. SYSTEM OVERVIEW

The block diagram of the 50KW FC is shown in Fig. 2. The charger is connected to a three phase four wire 380V AC distribution grid. The input stage comprises a three-phase diode rectifier, enforced by three single phase APF as a PFC circuit. Each APF is connected between a power phase and the neutral line. The current, drawn by the rectifier (i_{DR} for the R phase) is created by summation of the grid (i_R for the R phase) and APF (i_{FR} for the R phase) currents. The THD of the current, drawn by a three-phase diode rectifier with a resistive load (which is approximately the case in the FC) is around 31%. Therefore, taking into consideration a unity displacement factor, the power factor is way below the 92%, required by the regulation. Hence the APF should supply as much as possible of the rectifier current harmonic content, leaving the utility to supply mainly the first harmonic. The active power filters employ an independent control board, executing a control related to the grid requirements only, independent on the charging mode and power.

The rectified voltage v_{IN} is supplied directly to the output stage (note that there is no DC capacitor inserted between the stages). The output stage comprises twelve 4.5KW buck DC-DC converters, connected in parallel. The DC-DC converters are operated in an interleaving mode, divided into six groups of two converters, allowing significant reduction of both input and output currents of the DC-DC stage i_{IN} and i_O , respectively. A single output capacitor is connected at the charger output to further smooth the output current and allow output voltage adjustment prior to battery charging.



In order to prevent an uncontrolled current flow, the charger and the battery are separated by contactors. The DC-DC converters control board executes a dual level control algorithm. The high level algorithm creates voltage/current reference commands according to the desired charging mode, while the low level algorithm operates the DC-DC converters according to the high level control commands in an interleaved fashion. The detailed description of the hardware and the low level control is presented in the next sessions.

III. ACTIVE POWER FILTER OPERATION

A single phase APF, employed in the input stage of the FC, is shown in Fig. 3. The APF is implemented as a four quadrant DC-AC buck converter, connected to the utility via an inductor. Since the APF supplies reactive power only, single capacitor at the DC side is sufficient. However, since there are some power losses in the APF, the power balance of the capacitor must be ensured by a respective control loop in order to compensate the losses in the APF by drawing a small amount of active power from the utility. The outer control loop operates to maintain the power balance by keeping a constant DC link voltage at a level above the line voltage. The inner loop implements an indirect current control, i.e. instead of the filter current the utility current is sampled and controlled.

Recall that the utility reference current should be in phase with the utility voltage and have the same shape, while its magnitude should be equal to the first harmonic magnitude. The output of the power balancing loop sets the utility current magnitude while the sinusoidal shape is achieved by sampling the utility voltage and forcing the current loop reference current to follow it.

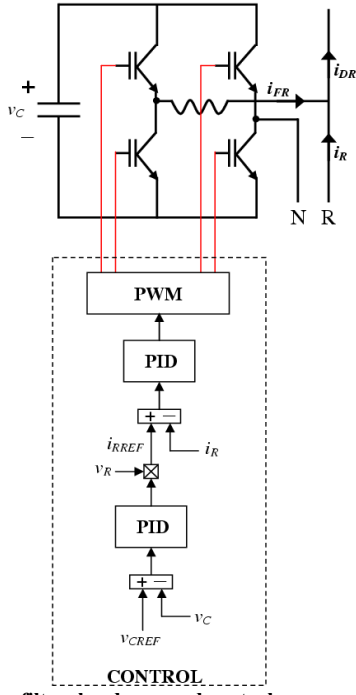


Fig. 3: Active power filter: hardware and control

IV. OUTPUT STAGE OPERATION

The output stage of the FC is shown in Fig. 4. As mentioned, it comprises six parallel buck cells, operated in an interleaved manner. Each cell is composed of two in-phase operated parallel buck converters, as shown in Fig. 5. The main loop of the output stage controls both the output current and voltage of the FC. The control command to each buck cell is the same and chosen according to the charging mode CC/CV. In order to implement an interleaved operation, the PWM clock to each buck cell is shifted by one-sixth of the PWM switching period D.

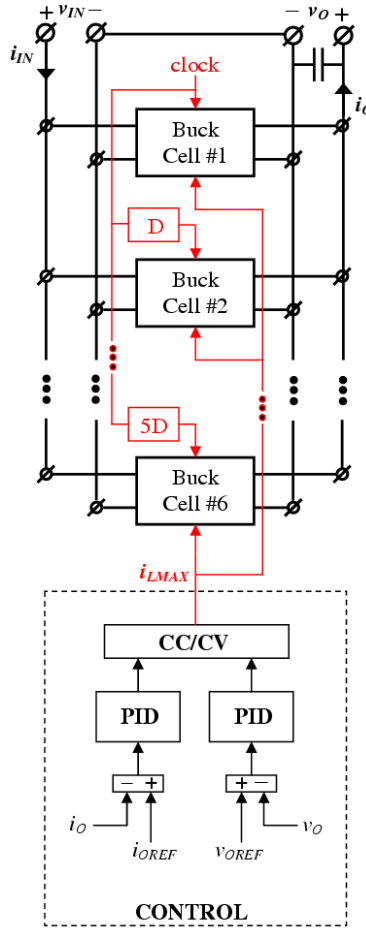


Fig. 4: Output stage overview and control

Each DC-DC converter contains a parallel MOSFET-IGBT pair as the switching device. Such a configuration allows benefiting from each transistor advantage: fast MOSFET turn-on time and low conduction losses of the IGBT. The output current of each buck cell is controlled utilizing a peak current mode control strategy, allowing both high-bandwidth current control and cycle-by-cycle current limit protection. All the buck cells employ similar control circuitry, since the interleaving is achieved by shifting the clock signals, supplied to the current mode control (CMC) blocks. An addition subcircuit controls the on/off timing of the MOSFET-IGBT pair.

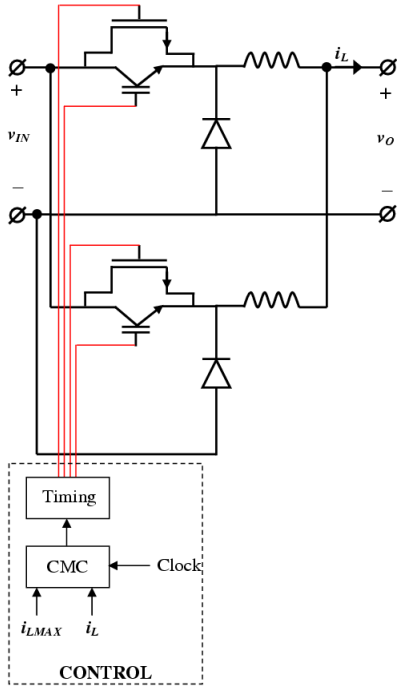


Fig. 5: Buck cell: hardware and control

V. SIMULATION RESULTS AND DISCUSSION

In order to validate the proposed design, the system was modeled and simulated using PSIM software. The input stage performance is shown in Fig. 6. Despite the highly nonlinear currents i_D drawn by the diode rectifier, the utility currents i_S are nearly sinusoidal and in phase with the utility voltages v_S , since the APF supplies the harmonic content i_F of the rectifier currents i_D . In order to emphasize the filtering function of the APF, the R phase spectra of the utility, rectifier and APF currents are shown in Fig. 7. Note the harmonic content of the diode rectifier currents, concentrated at $6n \pm 1$ harmonic, supplied by the APF, leaving the utility current spectra to contain energy mainly at first harmonic.

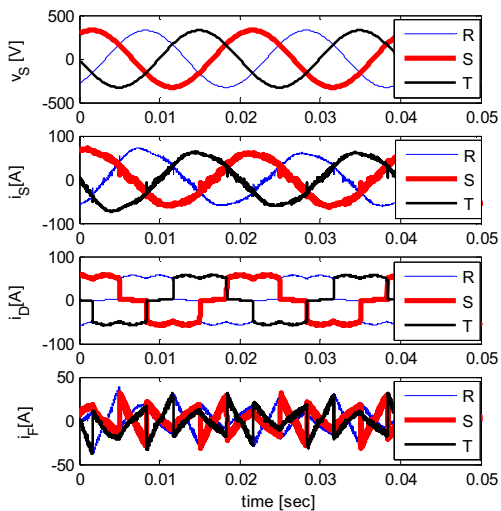


Fig. 6: Input stage performance

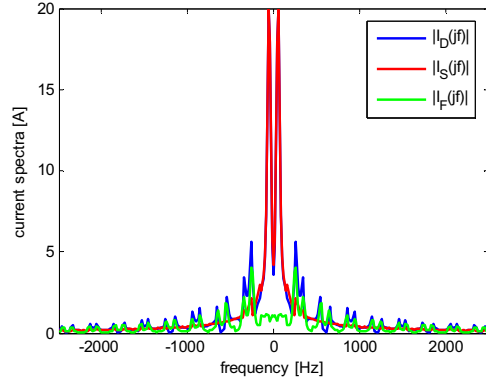


Fig. 7: The R phase spectra of the utility, rectifier and APF currents

The output stage performance is shown in Fig. 8 for a 45KW charging of at CC mode of 119A. Note the highly smooth transient performance and a stable steady-state operation. Despite the current ripple of nearly 5A of each buck cell, the interleaved operation causes the output current ripple to be as low as 0.8A, as shown in Fig. 9. In addition, even though the input current of each buck cell is highly discontinuous, ramping from zero at each switching cycle, the interleaved operation smoothes the total input current i_{IN} to an acceptable ripple level of 20%.

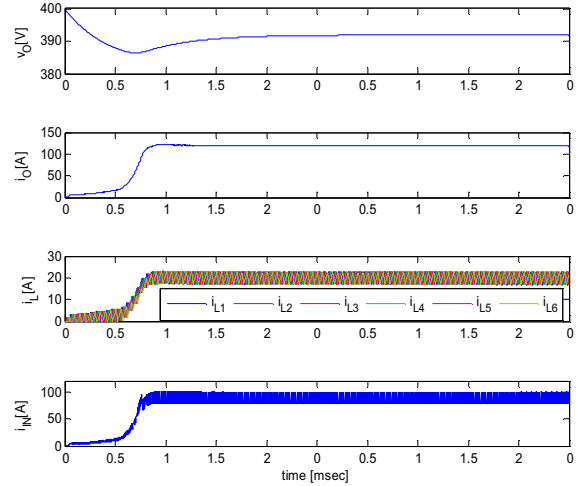


Fig. 8: Output stage performance

VI. CONCLUSION

A 50KW Li-Ion traction battery fast charger design was presented in the paper. The charger is a two-stage voltage power supply with dynamically controlled current limit function. The input stage includes a diode rectifier with a shunt connected active filter, achieving excellent results in terms of THD and power factor. The output stage is formed by six interleaved groups of two parallel connected buck DC-DC converters, employing current and voltage control according to the charging mode. The simulation results

enforce the proposed design by showing extremely promising results

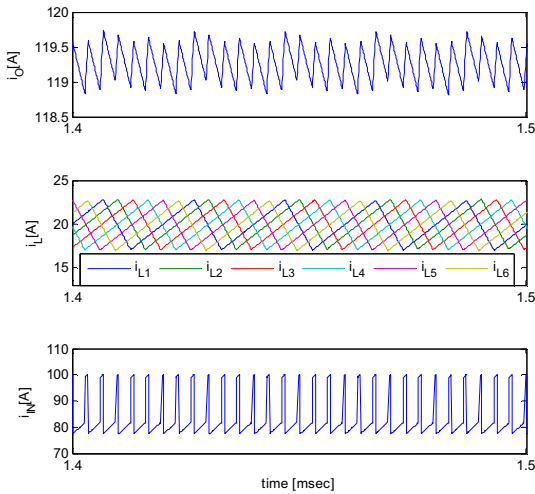


Fig. 8: Output stage zoomed currents

REFERENCES

- [1] B. Kennedy, D. Patterson and S. Camilleri, "Use of lithium-ion batteries in electric vehicles," *J. Pow. Sources*, vol. 90, pp. 156 – 162, 2000.
- [2] R. Gitzendanner, F. Puglia, C. Martin, D. Carmen, E. Jones and S. Eaves, "High power and high energy lithium-ion batteries for underwater vehicles," *J. Pow. Sources*, vol. 136, pp. 416 – 418, 2004.
- [3] G-C. Hsieh, L-R. Chen and K-S. Huang, "Fuzzy-controlled Li-Ion battery charge system with active state-of-charge controller," *IEEE Trans. Ind. Elec.*, vol. 48(3), pp. 585 – 593, 2001.
- [4] M. Chen and G. Rincon-Mora, "Accurate, compact, and power-efficient Li-Ion battery charger circuit," *IEEE Trans. Circ. Sys. II: Expr. Briefs*, vol. 53(11), pp. 1180 – 1184, 2006.
- [5] K. Tsang and W. Chan, "A simple and low-cost charger for lithium-ion batteries," *J. Pow. Sources*, vol. 191, pp. 633 – 635, 2009.
- [6] J-J Chen, F-C. Yang, C-C. Lai, Y-S. Hwang and R-G. Lee, "A high-efficiency multimode Li-Ion battery charger with variable current source and controlling previous stage supply voltage," *IEEE Trans. Ind. Elec.*, vol. 56(7), pp. 2469 – 2478, 2009.
- [7] D. Thimmesch, "An SCR inverter with an integral battery charger for electric vehicles," *IEEE Trans. Ind. Appl.*, vol. IA-21(4), pp. 1023 – 1029, 1985.
- [8] J. Bendien, G. Fregien and J. van Wyk, "High-efficiency on-board battery charger with transformer isolation, sinusoidal input current and maximum power factor," *IEE Proc. B*, vol. 133(4), pp. 197 – 204, 1986.
- [9] S-K. Sul and S-J. Lee, "An integral battery charger for four-wheel drive electric vehicle," *IEEE Trans. Ind. Appl.*, vol. IA-21(4), pp. 1023 – 1029, 1995.
- [10] B. Masserant and T. Stuart, "A maximum power transfer battery charger for electric vehicles," *IEEE Trans. Aerosp. Elec. Sys.*, vol. 33(3), pp. 930 – 938, 1997.
- [11] D. Jackson, A. Schultz, S. Leeb, A. Mitwalli, G. Verghese and S. Shaw, "A multirate digital controller for a 1.5KW electric vehicle battery charger," *IEEE Trans. Pow. Elec.*, vol. 12(6), pp. 1000 – 1006, 1997.
- [12] L. Solero, "Nonconventional on-board charger for electric vehicle propulsion batteries," *IEEE Trans. Veh. Tech.*, vol. 50(1), pp. 144 – 149, 2001.
- [13] M. Egan, D. O'Sullivan, J. Hayes, M. Willers and C. Henze, "Power-factor-corrected single-stage inductive charger for electric vehicle batteries," *IEEE Trans. Ind. Elec.*, vol. 54(2), pp. 1217 – 1226, 2007.
- [14] G. Pellegrino, E. Armando and P. Guglielmi, "An integral battery charger with power factor correction for electric scooter," *IEEE Trans. Pow. Elec.*, vol. 25(3), pp. 751 – 759, 2010.
- [15] N. Kutkut, D. Divan, D. Novotny and R. Marion, "Design considerations and topology selection for a 120KW IGBT converter for EV fast charging," *IEEE Trans. Pow. Elec.*, vol. 13(1), pp. 169 – 178, 1998.
- [16] C-H. Lin, C-Y. Hsieh and K-H. Chen, "A Li-Ion battery charger with smooth control circuit and built-in resistance compensator for achieving stable and fast charging," *IEEE Trans. Circ. Sys. I: Reg. Pap.*, vol. 57(2), pp. 506 – 517, 2010.
- [17] J. Orr, A. Emanuel and K. Oberg, "Current harmonics generated by a cluster of electric vehicle battery chargers," *IEEE Trans. PAS*, vol. PAS-101(3), pp. 691 – 700, 1982.
- [18] J. Orr, A. Emanuel and D. Pileggi, "Current harmonics, voltage distortion and powers associated with battery chargers," *IEEE Trans. PAS*, vol. PAS-101(8), pp. 2703 – 2710, 1982.
- [19] J. Orr, A. Emanuel and D. Pileggi, "Current harmonics, voltage distortion and powers associated with battery chargers distributed on the residential power system," *IEEE Trans. Ind. Appl.*, vol. IA-20(4), pp. 727 – 734, 1984.
- [20] S. Rahman and G. Shrestha, "An investigation into the impact of electric vehicle load on the electric utility distribution system," *IEEE Trans. Pow. Del.*, vol. 8(2), pp. 591 – 597, 1993.
- [21] P. Staats, W. Grady, A. Arapostathis and R. Thallam, "A statistical method for predicting the net harmonic currents generated by a concentration of electric vehicle battery chargers," *IEEE Trans. Pow. Del.*, vol. 12(3), pp. 1258 – 1266, 1997.
- [22] P. Staats, W. Grady, A. Arapostathis and R. Thallam, "A statistical analysis of the effect of electric vehicle battery charging on distribution system harmonic voltages," *IEEE Trans. Pow. Del.*, vol. 13(2), pp. 640 – 646, 1998.
- [23] J. Gomez and M. Morcos, "Impact of EV battery chargers on the power quality of distribution systems," *IEEE Trans. Pow. Del.*, vol. 18(3), pp. 975 – 981, 2003.
- [24] G. Gong, M. Heldwein, U. Drofenik, J. Minibock, K. Mino and J. Kolar, "Comparative evaluation of three-phase high-power-factor AC-DC converter concepts for application in future more electric aircraft," *IEEE Trans. Ind. Elec.*, vol. 52(3), pp. 727 – 737, 2005.
- [25] B-R. Lin and T-Y. Yang, "Three-phase AC/DC converter with high power factor," *IEE Proc. Electr. Power Appl.*, vol. 152(3), pp. 757 – 764, 2005.
- [26] M. Hartmann, S. Round, H. Ertl and J. Kolar, "Digital current controller for a 1MHz, 10KW three-phase VIENNA rectifier," *IEEE Trans. Pow. Elec.*, vol. 24(11), pp. 2496 – 2508, 2009.
- [27] K. Raggi, T. Nussbaumer, G. Doerig, J. Biela and J. Kolar, "Comprehensive design and optimization of a high-power-density single-phase boost PFC," *IEEE Trans. Ind. Elec.*, vol. 56(7), pp. 2574 – 2587, 2009.
- [28] J. Hahn, P. Enjeti and I. Pitel, "A new three phase power factor correction (PFC) scheme using two single phase PFC modules," *IEEE Trans. Ind. Appl.*, vol. 38(1), pp. 123 – 130, 2002.
- [29] H. Akagi, A. Nabae and S. Atoh, "Control strategy of active power filters using multiple voltage source PWM converters," *IEEE Trans. Ind. Appl.*, vol. IA-22(3), pp. 460 – 465, 1986.
- [30] J. Nastran, R. Cajhen, M. Seliger and P. Jereb, "Active power filter for nonlinear AC loads," *IEEE Trans. Pow. Elec.*, vol. 9(1), pp. 92 – 96, 1994.
- [31] D. Pedder, A. Brown, J. Ross and A. Williams, "A parallel-connected active filter for the reduction of supply current distortion," *IEEE Trans. Ind. Elec.*, vol. 47(5), pp. 1108 – 1117, 2000.
- [32] S. Kim, M. Todorovic and P. Enjeti, "Three-phase active harmonic rectifier (AHR) to improve utility input current THD in telecommunication power distribution system," *IEEE Trans. Ind. Appl.*, vol. 39(5), pp. 1414 – 1421, 2003.
- [33] H-L. Jou, J-C. Wu and H-Y. Chu, "New single-phase active power filter," *IEE Proc. Electr. Pow. Appl.*, vol. 141(3), pp. 129 – 134, 1994.
- [34] C. Hsu and H. Wu, "A new single-phase active power filter with reduced energy-storage capacity," *IEE Proc. Electr. Pow. Appl.*, vol. 143(1), pp. 25 – 30, 1996.
- [35] H. Komurcugil and O. Kukrer, "A new control strategy for single phase shunt active power filters using a Lyapunov function," *IEEE Trans. Ind. Elec.*, vol. 53(1), pp. 305 – 312, 2006.
- [36] C. Chang and M. Knights, "Interleaving technique in distributed power conversion systems," *IEEE Trans. Circ. Sys. I: Fund. Theory Appl.*, vol. 42(5), pp. 245 – 251, 1995.
- [37] D. Perreault and J. Kassakian, "Distributed interleaving of paralleled power converters," *IEEE Trans. Circ. Sys. I: Fund. Theory Appl.*, vol. 44(8), pp. 728 – 734, 1997.